

RESEARCH AND EDUCATION

Conventional and digital complete-arch implant impression techniques: An in vitro study comparing accuracy

Miguel Gómez-Polo, DDS, PhD,^a Alessandro Sallorenzo, DDS,^b Rocío Cascos, DDS,^c Juan Ballesteros, DDS,^d Abdul B. Barmak, MD, MSc, EdD,^e and Marta Revilla-León, DDS, MSD, PhD^f

ABSTRACT

Statement of problem. Varying complete-arch digital-implant-scanning techniques have been described, but their accuracy remains uncertain.

Purpose. The purpose of this in vitro investigation was to assess the effect of the implant angulation and impression method (conventional, intraoral digital scan, intraoral scan with a splinting framework, and combining cone beam computed tomography [CBCT] and intraoral scan) on the accuracy of complete arch implant recording.

Material and methods. The following 2 casts were obtained: one with 4 parallel (P group) and the other with 4 angled (up to 30 degrees) implant abutment analogs (NP group). Both the casts were digitized (7Series Scanner) (control file). The following 4 subgroups were created: conventional polyether impression with a splinted framework (CNV subgroup), intraoral scan (IOS subgroup), intraoral scan with a splinting framework (S-IOS subgroup), and intraoral scan combined with CBCT scan (CBCT-IOS subgroup) (n=10). For each file, an implant-supported bar was designed and imported into a program (Netfabb) to perform linear and angular interimplant abutment measurements. Two-way ANOVA (Analysis of Variance) and Tukey tests were selected to examine the data ($\alpha=.05$).

Results. Implant angulation ($P=.010$) and impression method ($P=.003$) significantly influenced the linear trueness. The P group (112 μm) obtained better linear trueness than the NP group (144 μm). The CNV subgroup obtained the best linear trueness, while the IOS and CBCT-IOS showed the worst trueness. Group ($P<.001$) significantly influenced angular trueness. Group ($P=.009$) and subgroup ($P<.001$) influenced the linear precision. The P group (72 μm) obtained better linear precision than the NP group (91 μm). The IOS subgroup obtained the best linear precision. Group ($P=.034$) significantly influenced the angular precision. The P group (0.46 degrees) had higher angular precision compared with the NP group (0.60 degrees).

Conclusions. Implant angulation and the impression methods tested, impacted the accuracy of the complete-arch implant recording. Parallel implants had better trueness and precision values than nonparallel implants. The conventional impression method showed the best trueness and precision. Among the digital implant scan methods assessed, the S-IOS and CBCT-IOS subgroups acquired significantly better trueness and precision than the IOS subgroup. (J Prosthet Dent 2022;■:■-■)

Intraoral scanners (IOSs) have been incorporated into dental procedures.¹⁻⁴ However, handling decisions such as IOS technology,⁵⁻⁷ ambient lighting conditions,⁸⁻¹⁰ ambient temperature changes,¹¹ length of the digital

Funding: This research did not receive any specific grant from funding agencies in the public, commercial, or not-for-profit sectors.

^aAssociate Professor, Department of Conservative Dentistry and Prosthodontics, School of Dentistry, Complutense University of Madrid, Madrid, Spain.

^bPhD Candidate and Postgraduate Resident in Advanced in Implant-Prosthodontics, Department of Conservative Dentistry and Prosthodontics, School of Dentistry, Complutense University of Madrid, Madrid, Spain.

^cPhD Candidate and Postgraduate Resident in Advanced in Implant-Prosthodontics, Department of Conservative Dentistry and Prosthodontics, School of Dentistry, Complutense University of Madrid, Madrid, Spain.

^dPrivate practice, Córdoba, Spain.

^eAssistant Professor, Clinical Research and Biostatistics Department, Eastman Institute of Oral Health, University of Rochester Medical Center, Rochester, NY.

^fAffiliate Assistant Professor, Graduate Prosthodontics, Department of Restorative Dentistry, School of Dentistry, University of Washington, Seattle, Wash and Faculty and Director of Research and Digital Dentistry, Koos Center, Seattle, Wash; Adjunct Professor, Department of Prosthodontics, School of Dental Medicine, Tufts University, Boston, Mass.

Clinical Implications

The accuracy of complete arch intraoral implant digital scans might be improved by implementing additional procedures, such as splinting frameworks or combining the scans with CBCT files, especially in unfavorable clinical situations such as when restoring angled implants.

scan,^{12,13} scanning protocol,^{14,15} clinician skills,¹⁶⁻¹⁸ and features of the surface digitized¹⁹⁻²² can affect the accuracy of intraoral scanning. Additionally, implant angulation²³⁻²⁷ and depth,²⁸ interimplant distance,²⁸⁻³¹ and implant-scan body design are factors that can also reduce scanning accuracy for implant-supported restorations.³⁰⁻³⁴

Diverse techniques have been described that aim to improve IOS scanning accuracy for implant-supported restorations, including splinting implant scan bodies and merging intraoral digital scans with cone beam computed tomography (CBCT) images.³⁵⁻⁴¹ However, the accuracy of these techniques for complete-arch digital scans remains unclear.

The objective of this investigation was to assess the effect of the implant angulation (parallel or angled up to 30 degrees) and recording method (conventional impression, intraoral digital scan, intraoral digital using a splinting framework, and intraoral digital scans combined with CBCT scans) on the trueness and precision of complete-arch implant-recording techniques. The null hypotheses were that the trueness and precision values of the complete-arch implant-recording methods tested with the different implant angulations assessed would not be significantly different.

MATERIAL AND METHODS

A completely edentulous maxillary cast was obtained. A computer-aided design (CAD) program (Dental Systems 2021, Model Builder; 3Shape A/S) was used to design 2 definitive casts (P and NP groups). An implant abutment analog (Transepithelial implant analog digital model; Avinent Implant System) was located in the right and left first molar, and right and left canine positions at the same apicocoronal height and 3 mm apical to the gingival margin of the diagnostic denture tooth arrangement. In the P group, the implant abutment analogs were placed parallel, while in the NP group, the implant abutment analogs were located with up to 30 degrees of angulation.

The virtual cast designs were fabricated by using a model resin (Nexdent Model 2.0 & Nexdent Gingiva Mask; 3D Systems) and a printer (Nexdent 5100; 3D Systems) according to the manufacturer's instructions. Subsequently, an implant abutment analog

(Transepithelial implant analog digital model; Avinent Implant System) was placed on each analog housing. The cast bases were filled with Type IV dental stone (GC Fujirock EP; GC) after mixing 100 g dental stone with 22 mL of water under vacuum for 30 seconds as per manufacturer recommendations. The casts were kept at 23 °C for 48 hours (Fig. 1).⁴²

A previously calibrated scanner (7Series Desktop Scanner; Dentalwings) was used to digitize the casts (P and NP groups) by following the manufacturer's protocol. First, a new implant abutment scan body (Transepithelial 4.8 scanbody; Avinent Implant System) was tightened to 15 Ncm (Torque wrench; Avinent Implant System) on each implant abutment analog by following the instructions of the manufacturer. Then, the reference or control files were acquired. The accuracy of the scanner was reported by the manufacturer to be 15 µm.

The following 4 subgroups were created depending on the complete-arch implant-recording method used to duplicate the definitive implant casts: conventional impression (CNV subgroup), intraoral digital scan (IOS subgroup), intraoral digital scan using a splinting framework (S-IOS subgroup), and intraoral digital scan combined with CBCT scan (CBCT-IOS subgroup) (Table 1).

For the P-CNV and NP-CNV subgroup specimens, a total of 10 splinted frameworks and 10 custom trays were fabricated by using light polymerizing composite resin material (Triad, clear; VOCO GmbH) (Fig. 2).⁴³ An implant impression abutment (Impression Coping 4.1 Open tray, Non-Engaging; Avinent Implant System) was tightened to 15 Ncm (Torque wrench; Avinent Implant System) on each implant abutment replica on the corresponding cast according to the manufacturer's endorsed protocol. Subsequently, a splinting framework was attached to the impression abutments with light-polymerizing acrylic resin (Conlight; Kuss dental).⁴³ Then, an open-tray polyether impression (Impregum Polyether Impression Material Penta; 3M ESPE) was obtained at room temperature.⁴⁴ The impression was poured with Type IV dental stone (GC Fujirock EP; GC). The cast was recovered after the dental stone had entirely set. These procedures were repeated until 10 specimens had been obtained in each subgroup.

For the P-IOS and NP-IOS subgroup specimens, a new implant scan body (Avinent Transepithelial 4.8 scanbody; Avinent Implant System) was placed and tightened to 15 Ncm (Torque wrench; Avinent Implant System) on each implant abutment analog, on each corresponding cast. The geometric bevel of the implant scan body was oriented toward the lingual surface.²⁶ A total of 10 successive digital scans were acquired by using an IOS (TRIOS 3, Pod, v. 1.7.19.0; 3Shape A/S) under controlled ambient lighting illumination of 1003 lux (Fig. 3).⁸⁻¹⁰ The device had been previously calibrated by

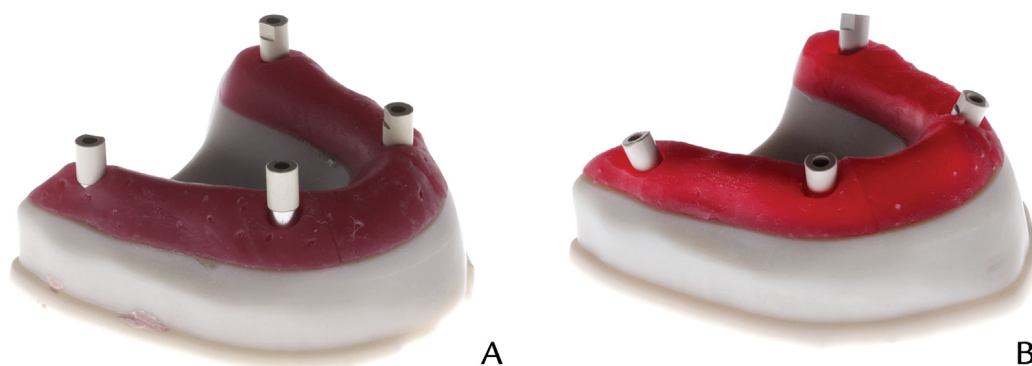


Figure 1. Definitive implant casts. A, P group. B, NP groups. NP, nonparallel; P, parallel.

following the manufacturer's protocol before the first scan of each subgroup.¹¹ All the IOS digital scans were acquired by a restorative dentist (M.G.-P.) with 8 years of previous experience with IOSs. The scanning protocol was performed by following a zigzag method.⁴⁵⁻⁴⁷ These procedures were repeated until 10 STL files or specimens had been obtained in each subgroup.

For the P-S-IOS and NP-S-IOS subgroups, 10 initial digital scans were captured by following the same methodology as for the P-IOS and NP-IOS subgroups. Then, 10 splinted frameworks (MedicalPlate; MedicalFit) were used by following the technique described by Gómez-Polo et al.⁴¹ Titanium abutments (Temporary Abutment Nonengaging; Avinent Implant System) were placed on the P and NP definitive implant casts to acquire the P-S-IOS and NP-S-IOS subgroup specimens. They were attached to the splinted framework with autopolymerizing acrylic resin (Conlight; Kuss dental). This procedure was repeated 10 times per subgroup (P-S-IOS and NP-S-IOS subgroups) to obtain 10 frameworks with splinted titanium abutments per group. A digital implant analog (ScAnalog; Dynamic Abutment) was attached to each titanium abutment, and each specimen was digitized by using the same IOS (TRIOS 3, Pod, v. 1.7.19.0; 3Shape A/S). Finally, each digitized scan of the titanium abutments was aligned with the initial intraoral scan to acquire the definitive P-S-IOS and NP-S-IOS file (Fig. 4).

For the P-CBCT-IOS and NP-CBCT-IOS subgroups, the digital scans were obtained by combining intraoral digital scans and CBCT images. A total of 10 consecutive CBCT (CS9300; Carestream Dental LLC) and IOS (TRIOS 3, Pod, v. 1.7.19.0; 3Shape A/S) scans were obtained. The intraoral scans were obtained by following the same protocol as in the P-CNV and NP-CNV subgroups. The corrected definitive implant cast was obtained by following the technique previously described by Gómez-Polo et al.³⁹ (Fig. 5).

The control file and experimental digital scans were imported into a software program (exocad v 2.2 Valetta; Align Technology). The implant scan bodies were aligned

Table 1. Characteristics of tested complete-arch implant recording methods

Group	Recording Method
CNV	Splinting framework Open custom tray Polyether impression material
IOS	Intraoral scanner (TRIOS 3, Pod, v. 1.7.19.0; 3Shape A/S)
S-IOS	Splinting framework (MedicalPlate; MedicalFit) Intraoral scanner (TRIOS 3, Pod, v. 1.7.19.0; 3Shape A/S)
CBCT-IOS	CBCT (CS9300; Carestream Dental LLC) Intraoral scanner (TRIOS 3, Pod, v. 1.7.19.0; 3Shape A/S)

CBCT, cone beam computed tomography; CNV, conventional; IOS, intraoral scanner; S, splinted.

using the corresponding implant scan body from the program library. An implant-supported bar was designed and exported in a standard tessellation language (STL) file format. Each implant-supported bar design was imported into a program (Netfabb, v. 2021; Autodesk) to obtain 6 linear interimplant abutment analog measurements and 3 angular calculations among the 4 implant abutment analogs. Trueness was outlined as the average discrepancy in implant position between the control file and experimental scans.^{26,48,49} Precision was defined as the measurement variations for each subgroup or standard deviation (SD).^{26,48,49}

The Shapiro-Wilk and Kolmogorov-Smirnov tests showed that the data were normally distributed ($P>.05$). Two-way ANOVA and the pairwise comparison Tukey tests were used to examine the trueness and precision data ($\alpha=.05$). All statistical analysis was accomplished by using a statistical software program (IBM SPSS Statistics for Windows, v26; IBM Corp).

RESULTS

The linear and angular trueness are described in Table 2. Regarding linear trueness evaluation, 2-way ANOVA showed that the groups (P and NP groups) ($df=1$, $MS=0.019712$, $F=6.98$, $Contribution=5.75\%$, $P=.010$) and subgroup (implant impression method) ($df=3$, $MS=0.04247$, $F=5.01$, $Contribution=12.92\%$, $P=.003$)

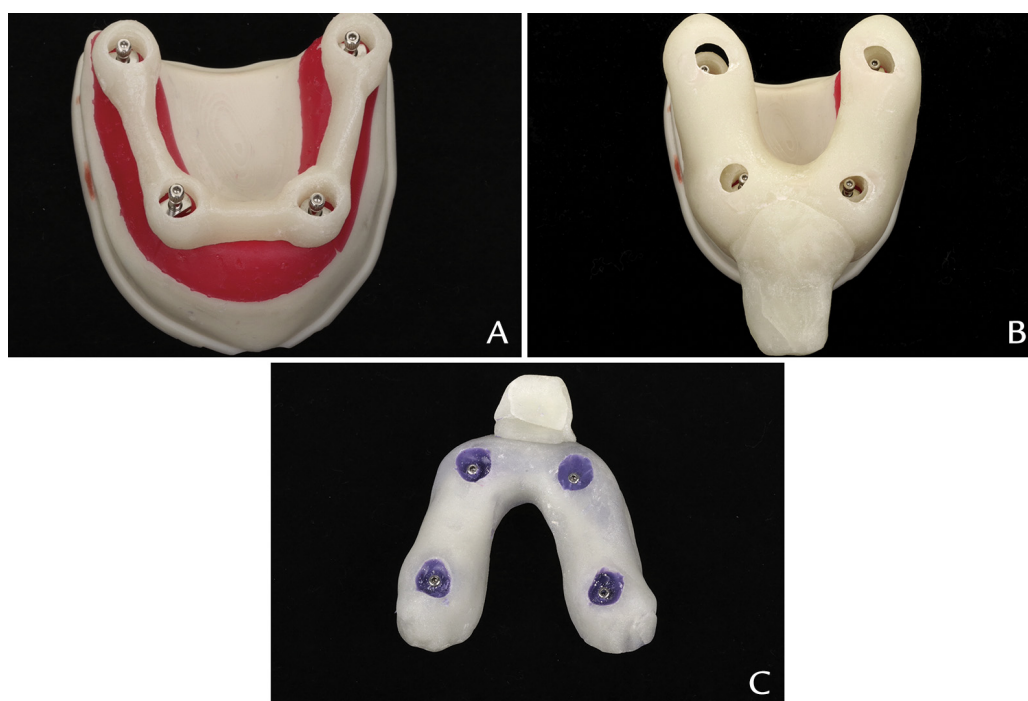


Figure 2. Representative conventional procedures (CNV subgroups). A, Splinting framework. B, Open-custom tray. C, Complete arch polyether implant impression.

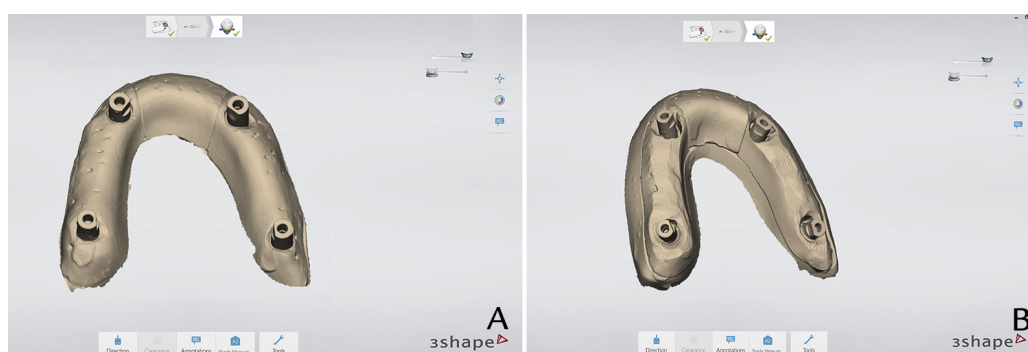


Figure 3. Representative intraoral digital scan (IOS subgroups). A, P group. B, NP groups. NP, nonparallel; P, parallel.

were significant factors in the linear trueness values obtained. A significant interaction between group and subgroup ($df=3$, $MS=0.07315$, $F=8.63$, $Contribution=21.73\%$, $P<.001$) was found (Fig. 6A).

With respect to the group factor, the Tukey pairwise comparison exhibited significant linear trueness value discrepancies among the tested groups. The P group ($112\ \mu m$) had higher linear trueness compared with the NP group ($144\ \mu m$). Additionally, the CNV subgroup had the highest linear trueness (lowest linear mean discrepancy) value, but the IOS and CBCT-IOS exhibited the lowest trueness (highest linear measurement discrepancy) value (Table 3). The linear trueness values of the CNV and S-IOS subgroups were not significantly different (Fig. 6B).

Regarding angular trueness evaluation, the 2-way ANOVA indicated that the group ($df=1$, $MS=10.8865$, $F=38.67$, $Contribution=31.89\%$, $P<.001$) was a significant factor in the angular trueness values obtained among the tested groups (Fig. 6C). The Tukey test exhibited no significant angular trueness differences among the different tested groups ($P>.05$) (Fig. 6D).

The linear and angular precision values are described in Table 4. Regarding linear precision evaluation, 2-way ANOVA indicated that the group ($df=1$, $MS=0.007765$, $F=7.22$, $Contribution=4.76\%$, $P=.009$) and subgroup ($df=3$, $MS=0.015846$, $F=14.74$, $Contribution=29.85\%$, $P<.001$) were significant factors in the linear precision values obtained among the tested groups. A significant

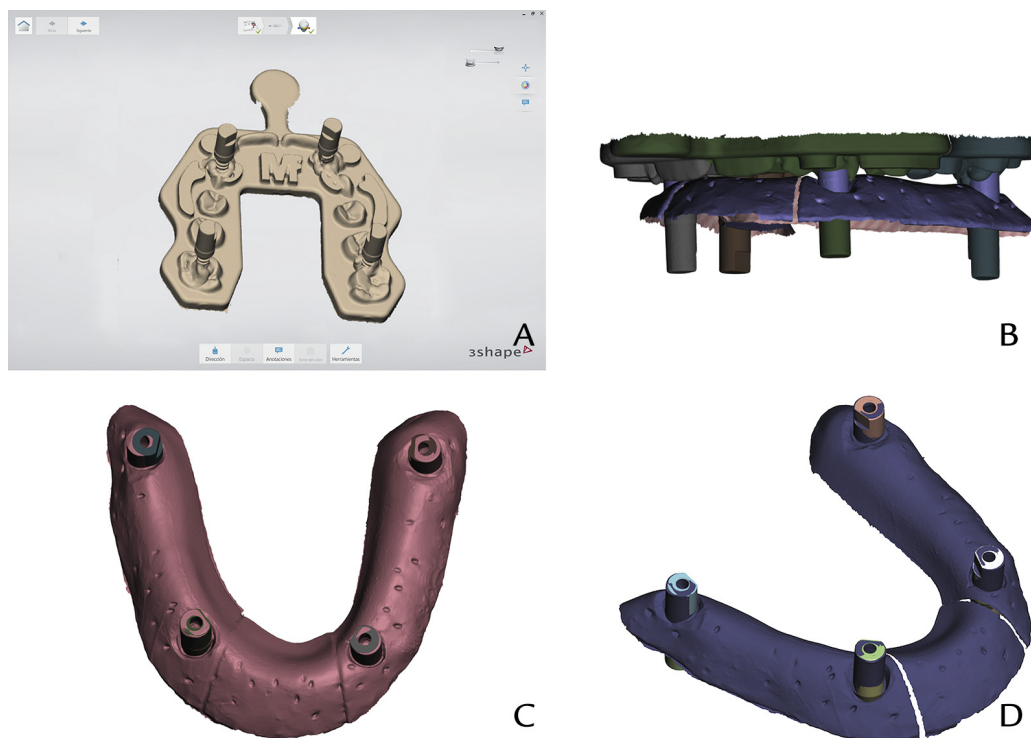


Figure 4. Representative intraoral digital scan with splinting framework (S-IOs subgroups). A, Scan of digital implant analogs screwed to titanium abutments and secured to scanning splint. B, Original scan superimposed to scanning splint considering implant positions. C, Deviations in scan body locations between original scan (pink) and scanning splint (gray). D, Definitive digital implant cast after segmentation of original scan based on scanning splint implant locations.

interaction between group and subgroup ($df=3$, $MS=0.009524$, $F=8.86$, $Contribution=17.81\%$, $P<.001$) was found (Fig. 7A). The Tukey multiple pairwise comparison test exhibited significant linear precision differences among the different groups evaluated. The P group ($72\ \mu m$) had higher linear precision compared with the NP group ($91\ \mu m$). The IOS subgroup had the highest mean discrepancies in linear precision among all the tested groups (Table 5) (Fig. 7B).

Regarding angular precision evaluation, the 2-way ANOVA showed that the group ($df=1$, $MS=0.41116$, $F=4.65$, $Contribution=5.16\%$, $P=.034$) was a significant factor in the angular precision obtained (Fig. 7C). The Tukey multiple pairwise comparison test indicated significant angular precision differences among the different tested groups. The P group had higher angular precision (0.46 degrees) than the NP group (0.60 degrees). The Tukey multiple pairwise comparison test revealed no significant differences in angular precision among the different subgroups assessed ($P>.05$) (Fig. 7D).

DISCUSSION

Based on the results of this investigation, parallel implants had significantly higher mean trueness and precision values than nonparallel implants. Additionally,

significant trueness and mean precision discrepancies were found among the tested, complete-arch implant-recording methods. Thus, the null hypotheses were rejected.

Previous investigations have examined the impact of implant angulation on IOS accuracy, reporting higher scanning accuracy with parallel implants.²³⁻²⁷ A recent systematic review assessed the effect of the implant position on the accuracy of complete arch implant recording techniques.²⁴ Eight in vitro investigations were included based on the inclusion criteria; however, 4 studies reported that implant angulation had no impact on intraoral scanning accuracy. Nonetheless, the remaining 4 studies did not provide information on implant angulation or on whether the definitive implant reference cast had the implant analogs positioned parallel.²⁴ The authors concluded that increased implant angulations (15 degrees) could impact IOS accuracy and that clinical studies were needed to comprehend the connection between implant angulation and IOS procedures.

Recent in vitro studies have reported higher trueness and mean values of precision on parallel implants when compared with angled implant positions, when performing complete arch intraoral digital scans.^{26,27} Similarly, this in vitro investigation revealed better trueness and mean values of precision with parallel implants compared with angled implants. Parallel implants had a

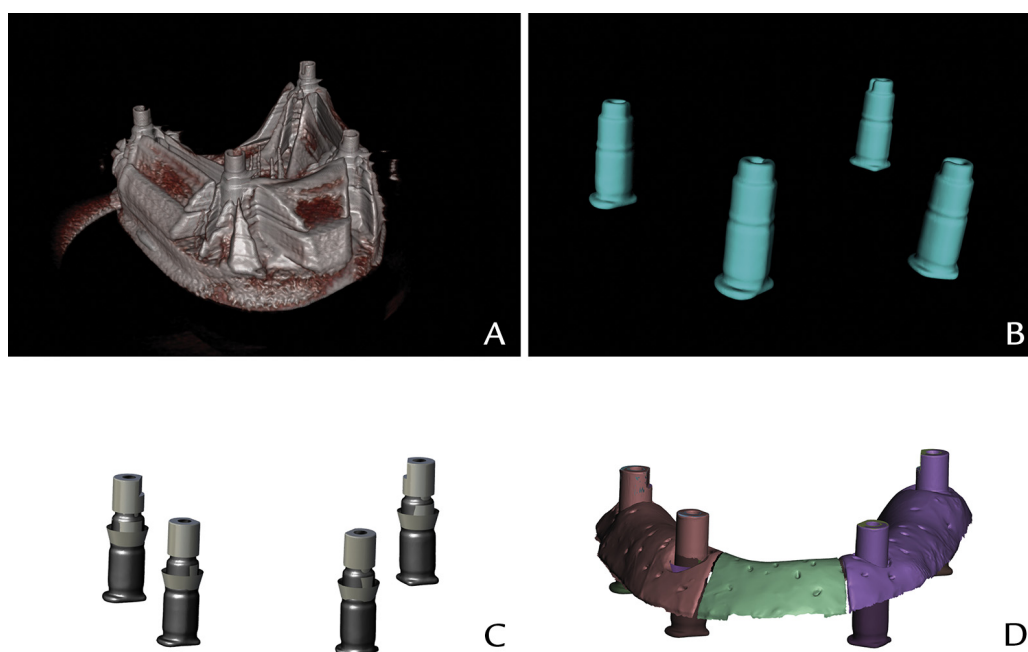


Figure 5. Representative intraoral digital scan combined with CBCT scan (CBCT-IOS subgroups). A, CBCT scan. B, Isolation of digital implants position from CBCT scan. C, Placement of digital scan bodies on implants from CBCT scan. D, Sectioning of original scan based on implant positions obtained with CBCT scan. CBCT, cone beam computed tomography.

Table 2. Trueness values for linear and angular measurement discrepancies obtained among different tested subgroups

Group	Subgroup	Mean \pm SD Linear Measurement Discrepancies (μ m)	Mean \pm SD Angular Measurement Discrepancies (degrees)
P	CNV	100 \pm 32	0.94 \pm 0.55
	IOS	96 \pm 36	0.68 \pm 0.23
	S-IOS	128 \pm 35	0.60 \pm 0.24
	CBCT-IOS	126 \pm 35	0.59 \pm 0.25
NP	CNV	99 \pm 70	1.36 \pm 0.94
	IOS	230 \pm 85	1.69 \pm 0.59
	S-IOS	108 \pm 56	1.17 \pm 0.54
	CBCT-IOS	140 \pm 49	1.54 \pm 0.51

CBCT, cone beam computed tomography; CNV, conventional; IOS, intraoral scanner; NP, non-parallel; P, parallel; S, splinted; SD, standard deviation.

linear trueness \pm precision mean value of 112 \pm 72 μ m and nonparallel implants (up to 30 degrees) 144 \pm 91 μ m, but no significant differences were measured between the 2 tested implant angulations. The results of the present study were consistent with those of previous publications; however, only the IOS subgroup could be directly compared because those research methodologies were similar.^{26,27}

In the present study, 4 different complete implant recording methods were compared. The conventional method had the best mean values of accuracy with a linear trueness \pm precision of 99 \pm 65 μ m and an angular trueness \pm precision of 1.15 \pm 0.53 degrees. Among the digital implant scanning methods assessed, the S-IOS and CBCT-IOS subgroups obtained significantly better

Table 3. Tukey post hoc multiple comparison results for linear trueness mean values obtained among tested subgroups

Subgroup	Mean Linear Measurement Discrepancies (μ m)
CNV	99 ^b
IOS	163 ^a
S-IOS	118 ^b
CBCT-IOS	133 ^{a,b}

CBCT, cone beam computed tomography; CNV, conventional; IOS, intraoral scanner; NP, non-parallel; S, splinted Means with different letters are significantly different ($P < .05$).

mean values of trueness and precision compared with the IOS subgroup. The S-IOS subgroup had a linear trueness \pm precision of 118 \pm 67 μ m and an angular trueness \pm precision of 0.88 \pm 0.49 degrees, while the CBCT-IOS subgroup had a linear trueness \pm precision of 133 \pm 71 μ m and an angular trueness \pm precision of 1.06 \pm 0.49 degrees. The worst accuracy values were computed in the IOS group with a linear trueness \pm precision of 163 \pm 124 μ m and an angular trueness \pm precision of 1.19 \pm 0.53 degrees, errors that were not clinically acceptable, indicating that the method cannot be recommended for complete-arch implant-digital scans.

Complete-arch intraoral scanning accuracy of different IOSs technologies has been evaluated,^{23-38,41} but limited information is available regarding the accuracy of CBCT images for acquiring implant position.^{39,40} The majority of studies have reported higher intraoral scanning accuracy when splinting the implant scan bodies compared with nonsplinting intraoral digital scan methods,^{23-38,41} consistent with the results of the present study.

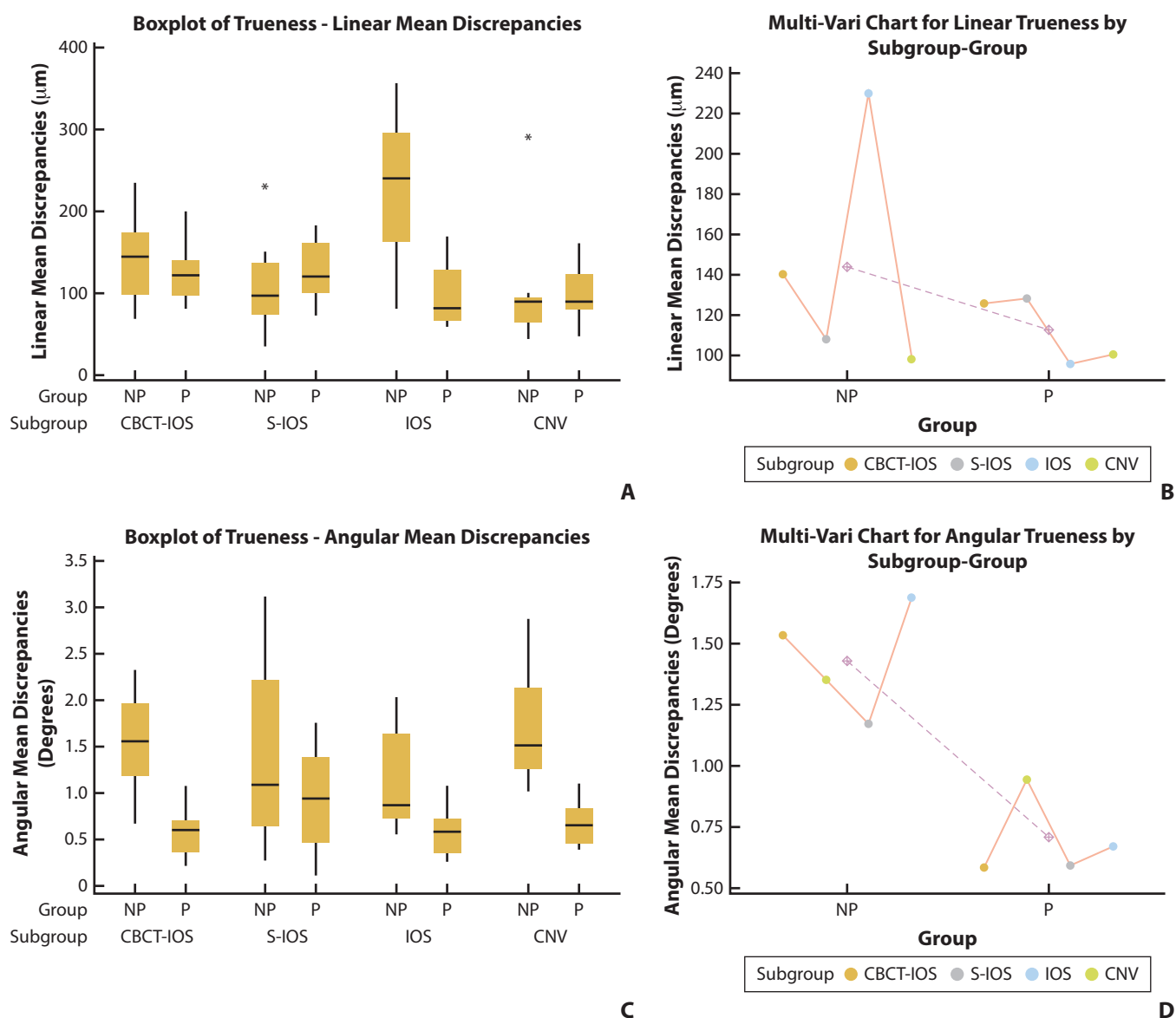


Figure 6. Trueness evaluation. A, Boxplot for linear measurement discrepancies. B, Multivari chart for linear discrepancy mean values by subgroup-group. C, Boxplot for angular measurement discrepancies. D, Multi-vari chart for angular discrepancy mean values by subgroup-group. CBCT, cone beam computed tomography; CNV, conventional; IOS, intraoral scanners; NP, nonparallel; P, parallel; S, splinted; SD, standard deviation.

Table 4. Precision values for linear and angular measurement discrepancies obtained among different tested subgroups

Group	Subgroup	Mean \pm SD Linear Measurement Discrepancies (μm)	Mean \pm SD Angular Measurement Discrepancies (degrees)
P	CNV	65 \pm 26	0.94 \pm 0.55
	IOS	82 \pm 45	0.68 \pm 0.23
	S-IOS	61 \pm 22	0.60 \pm 0.24
	CBCT-IOS	80 \pm 13	0.59 \pm 0.25
NP	CNV	66 \pm 37	1.36 \pm 0.94
	IOS	166 \pm 53	1.69 \pm 0.59
	S-IOS	72 \pm 27	1.17 \pm 0.54
	CBCT-IOS	64 \pm 14	1.54 \pm 0.51

CBCT, cone beam computed tomography; CNV, conventional; IOS, intraoral scanners; NP, non-parallel; P, parallel; S, splinted; SD, standard deviation.

Table 5. Tukey post hoc multiple comparison results for linear precision mean values obtained among tested subgroups

Subgroup	Mean Linear Measurement Discrepancies (μm)
CNV	65 ^b
IOS	124 ^a
S-IOS	67 ^b
CBCT-IOS	71 ^b

CBCT, cone beam computed tomography; CNV, conventional; IOS, intraoral scanner; NP, non-parallel; S, splinted. Means with different letters are significantly different ($P < .05$).

The accuracy of CBCT imaging for capturing the 3-dimensional implant position for fabricating complete-arch implant-supported prostheses was evaluated in a

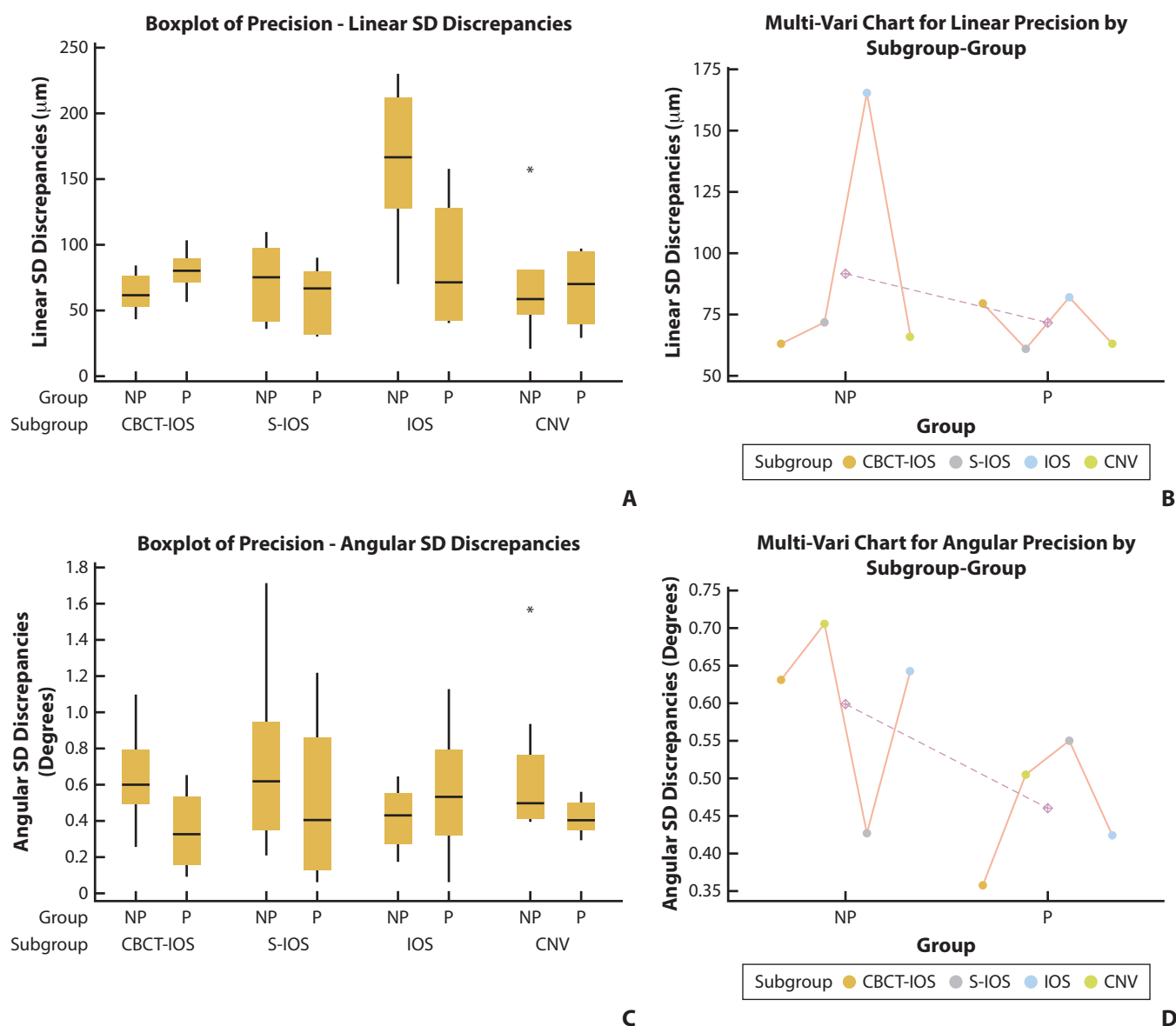


Figure 7. Precision evaluation. A, Boxplot for linear measurement discrepancies. B, Multi-vari chart for linear discrepancy mean values by subgroup-group. C, Boxplot for angular measurement discrepancies. D, Multi-vari chart for angular discrepancy mean values by subgroup-group. CBCT, cone beam computed tomography; CNV, conventional; IOS, intraoral scanners; NP, nonparallel; P, parallel; S, splinted; SD, standard deviation.

cadaver study.⁴⁰ Five implant-supported frameworks were manufactured with 6 implants per framework. Passive fit of the framework was assessed by 2 operators using a 1 to 10 scale related to the detection of screw-friction when seating the framework screws and direct clinical assessment with an explorer, and by assessing periapical radiographs and digital photography. The authors reported good fit on 3 frameworks and slight discrepancies on the remaining 2 specimens. However, the authors did not provide accuracy values for the tested digital scan; therefore, comparisons with this study were difficult.

Based on the results of this study, the S-IOS subgroup has statistically similar accuracy values to those of the CBCT-IOS subgroup ($P>.05$). However, the CBCT-IOS

technique requires radiation exposure. Nevertheless, additional in vitro and cadaver studies are necessary to assess the accuracy of the CBCT-IOS technique.

Limitations of this investigation included the in vitro experimental design and that a single IOS was used. Additionally, the conventional impressions of the CNV subgroups were obtained under room temperature conditions, which might have influenced the results obtained.⁴⁴ The thermal contraction of the impression material from mouth to room temperature was not modeled in the present study, making the conventional impression technique more accurate than it might be expected clinically.⁴⁴ Furthermore, the research methodology did not include the computer-aided design

(alignment between the implant scan body of the digital scan and the implant scan body of the CAD library) and manufacturing procedures (additive or subtractive methods) for fabricating complete-arch implant-supported prostheses. Therefore, higher discrepancies may occur when fabricating implant-supported prostheses. Clinical studies are suggested to further assess the impact of different complete arch implant recording techniques including IOSs and photogrammetry technologies.

CONCLUSIONS

Based on the findings of this in vitro study, the following conclusions were drawn:

1. The implant angulation and impression methods tested, influenced the accuracy of complete-arch implant-supported prostheses.
2. Parallel implant position exhibited significantly better trueness and precision mean values compared with nonparallel implant position (up to 30 degrees).
3. The conventional implant impression method showed the best trueness and precision mean values. Among the digital implant scanning methods assessed, the S-IOS and CBCT-IOS subgroups had significantly better trueness and precision mean values than the IOS subgroup.

REFERENCES

1. Tabesh M, Nejatidanesh F, Savabi G, Davoudi A, Savabi O, Mirmohammadi H. Marginal adaptation of zirconia complete-coverage fixed dental restorations made from digital scans or conventional impressions: a systematic review and meta-analysis. *J Prosthet Dent.* 2021;125:603–610.
2. Chochlidakis K, Papaspyridakos P, Tsigarida A, et al. Digital versus conventional full-arch implant impressions: a prospective study on 16 edentulous maxillae. *J Prosthodont.* 2020;29:281–286.
3. Giachetti L, Sarti C, Cinelli F, Russo DS. Accuracy of digital impressions in fixed prosthodontics: a systematic review of clinical studies. *Int J Prosthodont.* 2020;33:192–201.
4. Revilla-León M, Frazier K, da Costa JB, et al. Intraoral scanners: an American Dental Association Clinical Evaluators Panel survey. *J Am Dent Assoc.* 2021;152:669–670.e2.
5. Medina-Sotomayor P, Pascual-Moscaldó A, Camps I. Relationship between resolution and accuracy of four intraoral scanners in complete-arch impressions. *J Clin Exp Dent.* 2018;10:e361–e366.
6. Joda T, Zarone F, Ferrari M. The complete digital workflow in fixed prosthodontics: a systematic review. *BMC Oral Health.* 2017;17:124.
7. Renne W, Ludlow M, Fryml J, et al. Evaluation of the accuracy of 7 digital scanners: an in vitro analysis based on 3-dimensional comparisons. *J Prosthet Dent.* 2017;118:36–42.
8. Revilla-León M, Jiang P, Sadeghpour M, et al. Intraoral digital scans-part 1: influence of ambient scanning light conditions on the accuracy (trueness and precision) of different intraoral scanners. *J Prosthet Dent.* 2020;124:372–378.
9. Revilla-León M, Subramanian SG, Özcan M, Krishnamurthy VR. Clinical study of the influence of ambient light scanning conditions on the accuracy (trueness and precision) of an intraoral scanner. *J Prosthodont.* 2020;29:107–113.
10. Revilla-León M, Subramanian SG, Att W, Krishnamurthy VR. Analysis of different illuminance of the room lighting condition on the accuracy (trueness and precision) of an intraoral scanner. *J Prosthodont.* 2021;30:157–162.
11. Revilla-León M, Gohil A, Barmak AB, et al. Influence of ambient temperature changes on intraoral scanning accuracy. *J Prosthet Dent.* 21 February 2022. <https://doi.org/10.1016/j.prosdent.2022.01.012> [Epub ahead of print].
12. Moon YG, Lee KM. Comparison of the accuracy of intraoral scans between complete-arch scan and quadrant scan. *Prog Orthod.* 2020;21:36.
13. Kim MK, Son K, Yu BY, Lee KB. Effect of the volumetric dimensions of a complete arch on the accuracy of scanners. *J Adv Prosthodont.* 2020;12:361–368.
14. Oh KC, Park JM, Moon HS. Effects of scanning strategy and scanner type on the accuracy of intraoral scans: a new approach for assessing the accuracy of scanned data. *J Prosthodont.* 2020;29:518–523.
15. Müller P, Ender A, Joda T, Katsoulis J. Impact of digital intraoral scan strategies on the impression accuracy using the TRIOS Pod scanner. *Quintessence Int.* 2016;47:343–349.
16. Waldecker M, Rues S, Trebing C, Behnisch R, Rammelsberg P, Bömicke W. Effects of training on the execution of complete-arch scans. Part 2: scanning accuracy. *Int J Prosthodont.* 2021;34:27–36.
17. Lim JH, Park JM, Kim M, Heo SJ, Myung JY. Comparison of digital intraoral scanner reproducibility and image trueness considering repetitive experience. *J Prosthet Dent.* 2018;119:225–232.
18. Kim J, Park JM, Kim M, et al. Comparison of experience curves between two 3-dimensional intraoral scanners. *J Prosthet Dent.* 2016;116:221–230.
19. Shin SH, Yu HS, Cha JY, Kwon JS, Hwang CJ. Scanning accuracy of bracket features and slot base angle in different bracket materials by four intraoral scanners: an in vitro study. *Materials (Basel).* 2021;14:365.
20. Jin-Young Kim R, Benic GI, Park JM. Trueness of intraoral scanners in digitizing specific locations at the margin and intaglio surfaces of intracoronal preparations. *J Prosthet Dent.* 2021;126:779–786.
21. Anh JW, Park JM, Chun YS, Kim M, Kim M. A comparison of the precision of three-dimensional images acquired by 2 digital intraoral scanners: effects of tooth irregularity and scanning direction. *Korean J Orthod.* 2016;46:3–12.
22. Li H, Lyu P, Wang Y, Sun Y. Influence of object translucency on the scanning accuracy of a powder-free intraoral scanner: a laboratory study. *J Prosthet Dent.* 2017;117:93–101.
23. Basaki K, Alkumru H, De Souza G, Finer Y. Accuracy of digital vs conventional implant impression approach: a three-dimensional comparative in vitro analysis. *Int J Oral Maxillofac Implants.* 2017;32:792–799.
24. Carneiro Pereira AL, Medeiros VR, da Fonte Porto Carreiro A. Influence of implant position on the accuracy of intraoral scanning in fully edentulous arches: a systematic review. *J Prosthet Dent.* 2021;126:749–755.
25. Lin WS, Harris BT, Elathamna EN, Abdel-Azim T, Morton D. Effect of implant divergence on the accuracy of definitive casts created from traditional and digital implant-level impressions: an in vitro comparative study. *Int J Oral Maxillofac Implants.* 2015;30:102–109.
26. Gómez-Polo M, Álvarez F, Ortega R, et al. Influence of the implant scan body bevel location, implant angulation and position on intraoral scanning accuracy: an in vitro study. *J Dent.* 2022;121:104122.
27. Gómez-Polo M, Sallorenzo A, Ortega R, et al. Influence of implant angulation and clinical implant scan body height on the accuracy of complete arch intraoral digital scans. *J Prosthet Dent.* 22 March 2022. <https://doi.org/10.1016/j.prosdent.2021.11.018> [Epub ahead of print].
28. Zhang YJ, Shi JY, Qian SJ, Qiao SC, Lai HC. Accuracy of full-arch digital implant impressions taken using intraoral scanners and related variables: a systematic review. *Int J Oral Implantol (Berl).* 2021;14:157–179.
29. Choi YD, Lee KE, Mai HN, Lee DH. Effects of scan body exposure and operator on the accuracy of image matching of implant impressions with scan bodies. *J Prosthet Dent.* 2020;124:379.e1–379.e6.
30. Wulfman C, Naveau A, Rignon-Bret C. Digital scanning for complete-arch implant-supported restorations: a systematic review. *J Prosthet Dent.* 2020;124:161–167.
31. Zhang YJ, Shi JY, Qian SJ, Qiao SC, Lai HC. Accuracy of full-arch digital implant impressions taken using intraoral scanners and related variables: a systematic review. *Int J Oral Implantol (Berl).* 2021;14:157–179.
32. Carneiro Pereira AL, Medeiros VR, da Fonte Porto Carreiro A. Influence of implant position on the accuracy of intraoral scanning in fully edentulous arches: a systematic review. *J Prosthet Dent.* 2021;126:749–755.
33. Rutkūnas V, Gečiauskaitė A, Jeglevičius D, Vaitiekūnas M. Accuracy of digital implant impressions with intraoral scanners. A systematic review. *Eur J Oral Implantol.* 2017;10:101–120.
34. Motel C, Kirchner E, Adler W, Wichmann M, Matta RE. Impact of different scan bodies and scan strategies on the accuracy of digital implant impressions assessed with an intraoral scanner: an in vitro study. *J Prosthodont.* 2020;29:309–314.
35. Paratelli A, Vania S, Gómez-Polo C, Ortega R, Revilla-León M, Gómez-Polo M. Techniques to improve the accuracy of complete-arch implant intraoral digital scans: a systematic review. *J Prosthet Dent.* 27 October 2021. <https://doi.org/10.1016/j.prosdent.2021.08.018> [Epub ahead of print].
36. Iturrate M, Eguiraun H, Solaberrieta E. Accuracy of digital impressions for implant-supported complete-arch prosthesis, using an auxiliary geometry part-an in vitro study. *Clin Oral Implants Res.* 2019;30:1250–1258.
37. Roig E, Roig M, Garza LC, Costa S, Maia P, Espoña J. Fit of complete-arch implant-supported prostheses produced from an intraoral scan by using an auxiliary device and from an elastomeric impression: a pilot clinical trial. *J Prosthet Dent.* 2022;128:404–414.
38. Pan Y, Tsoi JKH, Lam WY, Zhao K, Pow EH. Improving intraoral implant scanning with a novel auxiliary device: an in-vitro study. *Clin Oral Implants Res.* 2021;32:1466–1473.

39. Gómez-Polo M, Ballesteros J, Padilla PP, Pulido PP, Revilla-León M, Ortega R. Merging intraoral scans and CBCT: a novel technique for improving the accuracy of 3D digital models for implant-supported complete-arch fixed dental prostheses. *Int J Comput Dent.* 2021;24: 117–123.
40. Corominas-Delgado C, Espona J, Lorente-Gascón M, Real-Voltas F, Roig M, Costa-Palau S. Digital implant impressions by cone-beam computerized tomography: a pilot study. *Clin Oral Implants Res.* 2016;27: 1407–1413.
41. Gómez-Polo M, Ballesteros J, Perales-Padilla P, Perales-Pulido P, Gómez-Polo C, Ortega R. Guided implant scanning: a procedure for improving the accuracy of implant-supported complete-arch fixed dental prostheses. *J Prosthet Dent.* 2020;124:135–139.
42. Schwedhelm ER, Lepe X. Fracture strength of type IV and type V die stone as a function of time. *J Prosthet Dent.* 1997;78:554–559.
43. Ma J, Rubenstein JE. Complete arch implant impression technique. *J Prosthet Dent.* 2012;107:405–410.
44. Kim KM, Lee JS, Kim KN, Shin SW. Dimensional changes of dental impression materials by thermal changes. *J Biomed Mater Res.* 2001;58: 217–220.
45. Kim RJ, Park JM, Shim JS. Accuracy of 9 intraoral scanners for complete-arch image acquisition: a qualitative and quantitative evaluation. *J Prosthet Dent.* 2018;120:895–903.e1.
46. Medina-Sotomayor P, Pascual-Moscardó A, Camps I. Accuracy of four digital scanners according to scanning strategy in complete-arch impressions. *PLoS One.* 2018;13, e0202916.
47. Mangano FG, Hauschild U, Veronesi G, Imburgia M, Mangano C, Admakin O. Trueness and precision of 5 intraoral scanners in the impressions of single and multiple implants: a comparative in vitro study. *BMC Oral Health.* 2019;19:101.
48. International Organization for Standardization. ISO 5725-1:1994. Accuracy (trueness and precision) of measurement methods and results - part 1: general principles and definitions. Available at: <https://www.iso.org/obp/ui/#iso:std:iso:5725:-1:ed-1:v1:en>.
49. International Organization for Standardization. ISO 20896-1:2019. Dentistry – digital impression devices – part 1: methods for assessing accuracy. Available at: <https://www.iso.org/standard/69402.html>.

Corresponding author:

Dr Marta Revilla-León
1001 Fairview Ave N # 2200
Seattle, WA 98109.
Email: marta.revilla.leon@gmail.com

Acknowledgments

The authors would like to thank Avinent Implant Systems for donating the implant analogs and transfers and the engineers and technicians of DentalEsthetic Dental Lab for their help in the models manufacturing.

Copyright © 2022 by the Editorial Council for *The Journal of Prosthetic Dentistry*.
<https://doi.org/10.1016/j.prosdent.2022.08.028>